buildings

MDPI

Article

The Effect of Smart Colored Windows on Visual Performance of Buildings

Negar Heidari Matin [1,*], Ali Eydgahi [2] and Payam Matin [3]

[1] Gibbs College of Architecture, University of Oklahoma, Norman, OK 73019, USA
[2] Gameabove College of Engineering & Technology, Eastern Michigan University, Ypsilanti, MI 48197, USA; aeydgahi@emich.edu
[3] Department of Engineering and Aviation Sciences, University of Maryland Eastern Shore, Princess Anne, MD 21853, USA; phmatin@umes.edu
* Correspondence: negar.matin@ou.edu

Abstract: The photochromic coating is a promising smart technology that provides different optical properties in response to daylight variations. The application of photochromic coatings with various colors/shades on window glass is one of the current research approaches for finding better energy saving techniques. The aim of this study was to develop a series of photochromic coatings for window glass and measure the impact of such smart technologies on occupants' visual comfort. This paper examines the visual performance of building facades that utilize windows with different photochromic-coated glass. The visual performance data of three window types coated with nine different photochromic color shades were considered and compared to determine the best photochromic shades and window types that provide optimum visual metrics for the inside of the building. The results show that compared to no-coating glass, both the Daylight Glare Probability and the Useful Daylight Illuminance could be improved by using multi-color coatings that contain equal or different color proportions for photochromic window glass. From an energy-saving point of view, the results indicate that the windows coated with photochromic materials provide a better alternative to the no-coating window products.

Keywords: smart colored windows; responsive facades; photochromic coating; visual comfort; building performance

Citation: Heidari Matin, N.; Eydgahi, A.; Matin, P. The Effect of Smart Colored Windows on Visual Performance of Buildings. *Buildings* **2022**, *12*, 861. https://doi.org/10.3390/buildings12060861

Academic Editors: Wei-Ling Hsu, Teen-Hang Meen, Hsi-Chi Yang and Wen-Der Yu

Received: 2 April 2022
Accepted: 10 June 2022
Published: 20 June 2022

1. Introduction

Materials that are able to significantly alter one or more of their inherent properties with the application of external stimuli such as stress, temperature, moisture, pH, electrical fields, and magnetic field, in a controlled fashion, are known as smart materials [1]. Applying smart materials as a smart coating on windows can improve energy efficiency, user comfort and well-being, and decrease CO_2 emissions in built environments [2]. Different types of smart coatings, such as electrochromic [3–5], thermochromic [6], gasochromic [7], and liquid crystal [8] have been utilized to develop smart windows [9–11]. The coating of photochromic materials can be applied on the surface of window glass as a thin film to provide a capability for the glass to dynamically adjust its own color, transparency, and consequently, its reflective properties upon exposure to various intensities of sunlight over a day [12]. It needs to be noted that the dynamic behavior of photochromic coatings is reversible and by dimming or blocking the sunlight the glass will revert to its initial optical properties [10]. As a result, the optical properties of photochromic coated windows countinouselly move between bleached phase and colored phase [13]. The dynamic behavior in response to sunlight intensities caused by such photochromic coatings could be a promising replacement for implemented mechanical and electro-mechanical technologies in the design and development of responsive facades [14].

A literature review of the most recent studies on smart windows is summarized in Table 1 [14–36]. Although the majority of studies examine the influence of thermochromic [19–26], electrochromic [27–30], and gasochromic coatings [31–33] on building energy consumption, CO_2 emission, heading, and cooling load [34–36], only a few studies has focused on the photochromic coating and its application in the built environment [14–18]. Additionally, among studies of smart windows with photochromic coatings, the effect of such coating on occupants' visual comfort has not been adequately explored. In addition, only three colors/shades of gray, blue, and green have been investigated and no investigation has focused on combinations of different photochromic colors/shades and their visual performance in buildings.

Table 1. A summary of literature review of the most recent studies on smart windows.

Ref. No.	Year	Authors	Coating Type	Dependent Variables	Method
[27]	2021	Cannavale et al.	Electrochromic	Building Energy Efficiency& Visual Comfort	Review
[31]	2021	Marchwiński	Gasochromic & electrochromic	Energy consumption	Simulation
[19]	2021	Liang et al.	Thermochromic	Visual comfort	questionnaires
[20]	2021	Wang et al.	Thermochromic	Energy efficiency cooling load	Laboratory
[21]	2021	Zoe et al.	photo-/electro-driven Thermochromic	Energy efficiency	Review
[14]	2021	Cannavale et al.	Photochromic	Energy efficiency	Laboratory & simulation
[32]	2020	Nageib et al.	Gasochromic, thermochromic & electrochromic	Energy consumption	Simulation
[22]	2020	Zhou et al.	Thermochromic	Energy consumption with heat storage	Laboratory & simulation
[23]	2019	Aburas et al.	Thermochromic	energy-saving performance, thermal & visual comfort	Review
[15]	2019	Tällberg et al.	Photochromic	Energy consumption	Simulation
[24]	2018	Cui et al.	Thermochromic	Energy-saving performance	Review
[16]	2018	Cao et al.	Photochromic	Energy consumption	Laboratory & simulation
[28]	2018	Granqvist et al.	Electrochromic	Energy efficiencywith good indoor comfort	Review
[17]	2017	Miyazaki et al.	Photochromic	Optical properties	Laboratory
[18]	2017	Zeng et al.	Photochromic	Energy performance	Review
[29]	2016	Rossi et al.	Electrochromic	energy saving and visual comfort	Laboratory & Physical experiment
[33]	2016	Feng et al.	Gasochromic & electrochromic	Energy consumption	Simulation
[30]	2015	Reynisson, H.	electrochromic	Energy consumption	Simulation
[25]	2015	Liang et al.	Thermocromich	Thermal comfort, Visual comfort, Energyconsumption	Simulation
[26]	2013	Kamalisarvestani et al.	Thermocromich	Energy-saving potentials and thermal comfort	Review

Thus, this study first focused on formulating a new series of photochromic coatings for window glass substrates in a laboratory environment and then evaluated their visual perfor-

mance in a building environment. The main colors that were developed for photochromic coatings included red, medium blue, yellow, and their dual and triple combinations. To assess the visual performance of window glass substrates, the Red-Green-Blue (RGB) values determination test was utilized to determine the optical properties of photochromic glass. Then, the obtained optical propertie's data were used to simulate the smart coated windows using validated daylight simulator software. Three smart window types were designed including one-layer photochromic glass, two-layer photochromic glass, and one-layer of low-e glass with one-layer of photochromic glass. The visual performance of the photochromic windows was evaluated using Daylight Glare Probability (DGP) and Useful Daylight Illuminance (UDI) [37]. An office room with a smart window as a facade was parametrically simulated to test the developed smart coated windowpanes for different color scenarios. The visual performance evaluations were repeated for south, east, north, and west orientations as the main facade directions during different hours and days. Then, to identify the best photochromic colors and windowpane types, the results were compared with a no-coating glass window.

2. Materials and Methods

2.1. Smart Color Coated Windowpane

The smart coatings were created by using photochromic dyes of red, medium blue, and yellow colors. Each dye solution was added to the mixture of thermoplastic acrylic resin and leveling agent additive. Table 2 lists the formulations of each coating color that was used. The coating materials were applied to the degreased glass plates and pre-coated low-carbon steel panels with a wet film thickness of 4 mils (100 µm) using a film applicator. The glass plates were exposed to a UV LED light lamp to check the photochromic activity of coatings. The applied coating materials were then left at ambient conditions for 24 h to dry.

Table 2. Photochromic coatings with different color compositions.

		Coating Compositions								
		Red Dye	**Medium Blue Dye**	**Yellow Dye**	**Thermoplastic Acrylic Resin**	**Additive**	**Solvent**	**Total (wt%)**	**Solid Content (wt%)**	**Dye Content (wt%)**
Photochromic Coating	Blank	0	0	0	62.2	0.1	37.7	100	24.98	0
	Red	0.25	0	0	61.65	0.1	38	100	25.01	1
	Medium Blue	0	0.25	0	61.65	0.1	38	100	25.01	1
	Yellow	0	0	0.25	61.65	0.1	38	100	25.01	1
	Red-Medium Blue	0.125	0.125	0	61.65	0.1	38.05	100	24.99	1
	Red-Yellow	0.125	0	0.125	61.65	0.1	38	100	25.01	1
	Medium Blue-Yellow	0	0.125	0.125	61.65	0.1	38	100	25.01	1
	Red-Medium Blue-Yellow	0.08	0.085	0.085	61.65	0.1	38	100	25.01	1

The photochromic coatings have reversible properties that adapt to glass light transmittance based on the amount of solar irradiance received [38,39]. Thus, to determine the light transmittance of the coated glass plates over time, the direct photographic technique was used to measure the RGB values of the coated glass plates. The direct photography was conducted for the two days of 25 May and 16 September at the two different times of 12:00 p.m. and 6:00 p.m., because the maximum solar radiation occurrs at 12:00 p.m. and the minimum happens at 6:00 p.m. [40,41]. Accordingly, the coated glass plates were initially exposed to direct sunlight for 60 s, before being placed in the gap between the diffuser and the guiding camera lens, and were instantly photographed. The RGB values of the coated glass were acquired after uploading the photographs to Adobe Photoshop.

The photochromic coatings applied to the glass plates showed high light transmittance at the bleached condition and significant low light transmittance at the colored conditions. Figure 1 demonstrates the glass plates coated with red, medium blue, and yellow colors with four different exposure times of 0, 10, 30, and 60 s.

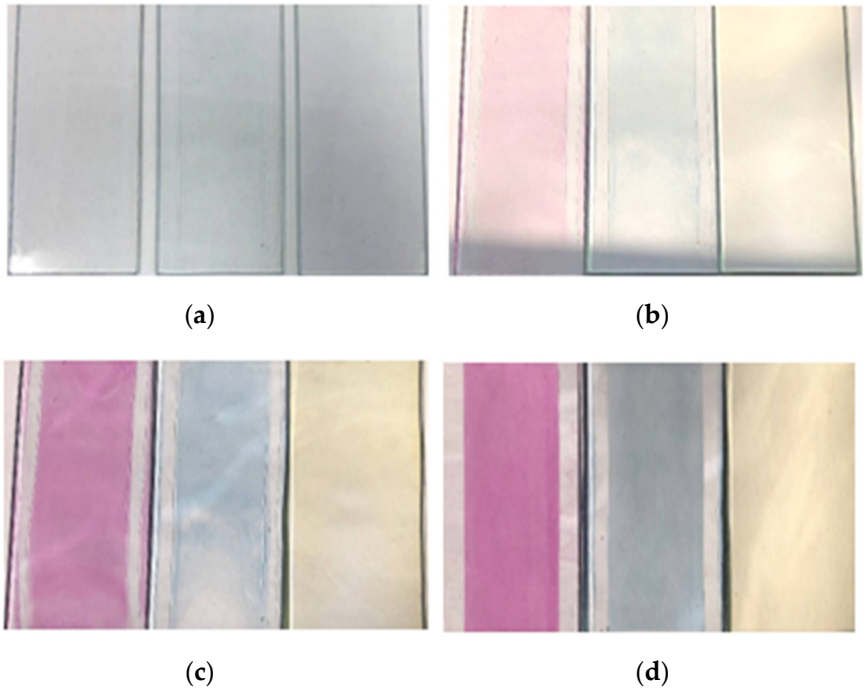

Figure 1. Glass plates coated with different color shades; (**a**) No sun exposure (**b**) 10-s sun exposure (**c**) 30-s sun exposure (**d**) 60-s sun exposure [39].

2.2. Simulation of the Building Smart with Color Coated Windowpane

A simple office room with the dimensions of 4.0 m wide, 9.0 m deep, and 3.0 m high was designed. A shoebox office model was chosen because the results are easily read and interpreted, and the effect of design parameters such as colored glass type, facade type, and window size can quickly be analyzed [40].The depth of the room was chosen to be larger than the typical depth so that the effect of daylight remains visible for all variants [41]. Natural light was considered the only light source in the office room with no artificial lighting. This simulated office room was designed to have a 2.6 m width and 3.6 m length window. A responsive facade system with a window was parametrically modeled and applied to the office room using the Grasshopper modeling tool. The simulated room could be rotated to face N, W, S, and E as the four main cardinal directions.

The office was assumed to be located in the city of Ann Arbor in Michigan and to be occupied daily from 8:00 a.m. to 6:00 p.m. outside of daylight savings time. The occupancy schedule was in agreement with IESNA's new Lighting Measurement IES LM-83–12 [41]. During occupancy hours, it was assumed that six workspaces were occupied, and occupants were performing regular office work, including working on a computer. The clear sky with the sun was considered as the sky conditions. The weather data for the office location was obtained from the U.S. Department of Energy that provides typical annual meteorological data as an EnergyPlus Weather File (EPW).

For the office room, a Grasshopper plug-in for Rhinoceros software was utilized to simulate one-pane and two-pane photochromic coated glass windows. The data obtained from the RGB determination test was used by the Honeybee Legacy plug-in for Grasshopper to characterize each of the ten color shades used in photochromic glass windows. The honeybee Legacy is one of Grasshopper's plug-ins, which assists Grasshopper to conduct sustainability simulations, such as daylight analysis using Radiance engine. Radiance is

software that was numerously validated previously by other researchers [42–45]. Reinhart and Walkenhorst [42] have shown that Radiance-based simulation methods "are able to efficiently and accurately model complicated daylighting elements such as Venetian blind system". Additionally, Reinhart and Andersen [43] have shown that translucent materials "can be modeled in Radiance with an even higher accuracy than what was demonstrated in the earlier studies". Statistic software R and Microsoft Excel were utilized for the management, visualization and analysis of the data.

The Honeybee Legacy plug-in was utilized to measure DGP and hourly usable daylight illuminance (UDI_h). As a grid-based metric, UDI_h was measured by defining 900 sensors located over a horizontal grid surface with a height of 0.83 m from the office floor, which was within the standard of the height for work-plane surfaces in an office area. The sensors were spaced approximately every 0.2 m from each other in both surface directions. The interior of the office room was simulated with standard radiance materials that included a generic floor with 20% reflectance, a generic ceiling with 70% reflectance, generic interior walls with 50% reflectance, and generic furniture with 50% reflectance to allow indirect illumination.

DGP is classified in four ranges of 0–35 (imperceptible), 35–40 (perceptible), 40–45 (disturbing), and 45–100 (intolerable) [46]. To calculate DGP, a camera needs to be located in the simulated office at the eye level of an assumed occupant seated behind a workstation working with a computer. In this study, the camera was located at the first workstation on the right side of the window facing the cardinal directions. It needs to be noted that the DGP calculations are based on a formula developed by Wienold and Christofferen as follows [46]:

$$DGP = c_1 E_v + c_2 \log\left(1 + \sum_i \frac{L_{S,I}^2 w_{s,i}}{E_v^{a_1} P_i^2}\right) + c_3 \quad (1)$$

where E_v is the vertical eye illuminance (Lux), constant $c_1 = 5.87 \times 10^{-5}$; L_S is the luminance of the source (cd/m^2), constant $c_2 = 9.18 \times 10^{-2}$, w_s is the solid angle of the source, constant $c_3 = 0.16$; P is the position index, and constant $a_1 = 1.87$.

UDI_h is an indicator for evaluating the hourly light amount that exists in a specific interior space, which includes lower and upper thresholds and an acceptable range as $UDI_{underlit}$ (300 Lux < E), $UDI_{overlit}$ (E > 1000 Lux), and UDI_{useful} (300 Lux < E < 1000 Lux), respectively [47–52]. Calculating UDI_h can be considered as an attempt to integrate the measurement of indoor illuminance level and discomfort glare in one scheme [53,54]. In general, UDI_h is defined as a weighted average as follows [49]:

$$UDI = \frac{\sum_i (wf_i . t_i)}{\sum_i (t_i)} \quad (2)$$

where t_i is the time when the illuminance E is calculated, and wf_i is the weighting factor, which depends on the range of the calculated illuminance E. It should be noted that wf_i weighting factor is selected based on the range of the calculated illuminance E. For instance, as shown below, for the upper threshold, $UDI_{overlit}$ is calculated as below after wf_i is selected depending on how the illuminance E value is compared to the upper limit of illuminance specified in standards [49]:

$$UDI_{overall} \text{ with } wf_i = \begin{cases} 1 & \text{if } E > E_{Upper\ limit} \\ 0 & \text{if } E \leq E_{Upper\ limit} \end{cases} \quad (3)$$

In a similar way, the lower threshold $UDI_{underlit}$ is calculated as:

$$UDI_{Usefull} \text{ with } wf_i = \begin{cases} 1 & \text{if } E_{Lower\ limit} < E \leq E_{Upper\ limit} \\ 0 & \text{if } E \leq E_{Lower\ limit} \vee E > E_{Upper\ limit} \end{cases} \quad (4)$$

Similarly, UDI_{useful} is calculated as:

$$UDI_{Underlit} \text{ with } wf_i = \begin{cases} 1 & \text{if } E_{Daylight} < E_{Lowelimit} \\ 0 & \text{if } E_{Daylight} \geq E_{Lower\ limit} \end{cases} \quad (5)$$

3. Results and Discussion

3.1. Experiment Setting

The DGP and UDI_h are considered as the two main metrics of visual comfort of a building. The visual performance data of each photochromic color coated windows were studied and compared to determine the best photochromic shades for managing daylight inside the simulated office. To determine these metrics, three types of windows and ten different color coatings were utilized. The types of windows considered for testing were:

a Type A window, which consists of a one-layer photochromic glass,
b Type B window, which consists of two-layer photochromic glass,
c Type C window, which consists of one-layer of photochromic glass in interior and one-layer of Low-E glass in the exterior.

The color shades considered for each window types were:

1 Blank (no color coating),
2 Red color (R),
3 Medium Blue color (MB),
3 Medium Blue color (MB),
4 Yellow color (Y),
5 Combination of Red and Medium blue colors (RMB),
6 Combination of Red and Yellow colors (RY),
7 Combination of Medium blue and Yellow colors (MBY),
8 Combination of Red, Medium blue, and Yellow colors (RMBY),
9 Combination of 1/4 R, 1/4 MB, 1/4 MBY, and 1/4 Y colors (MCP),
10 Combination of 1/2 R, 1/6 MB, 1/6 Y, and 1/6 MBY (MCPs).

The architectural sketches of the color shades are presented in Figure 2. It needs to be noted that grasshopper scripts were utilized to randomly distribute the selected colors of R, MB, Y, and MBY on the surface of the windowpane with and without color proportions in order to create MCP and MCPs scenarios.

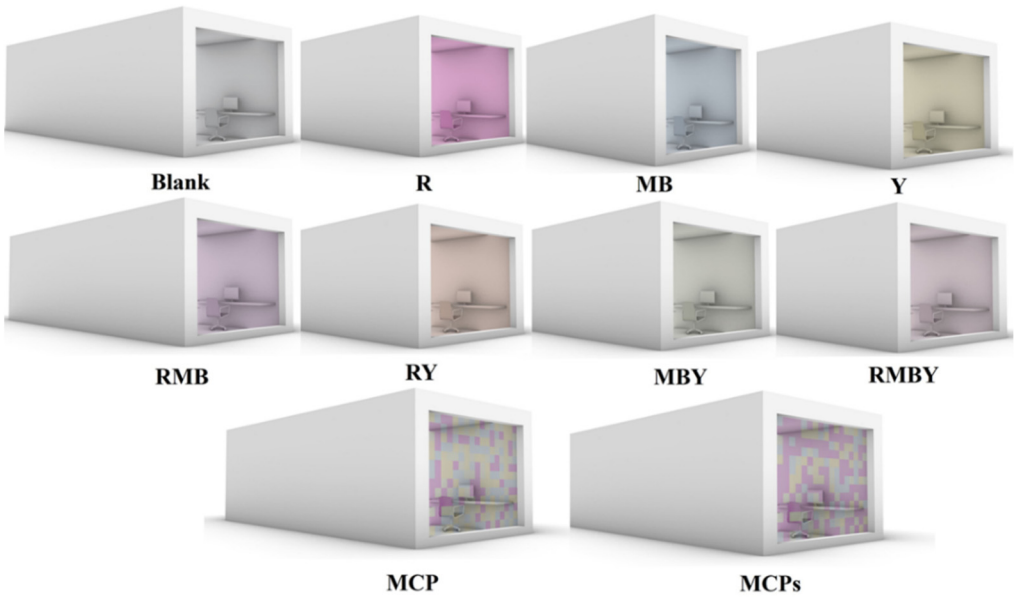

Figure 2. Coated color shades used for windows.

By using Honeybee software, DGP and UDI_h for all three window types with each of the ten color shades, for two days of 25 May and 16 September at two times of 12:00 p.m. and 6:00 p.m. were computed and reapeated for each of the four (N, S, W, and E) facade directions.

3.2. DGP Analysis

Figures 3 and 4 show the computed DGPs for 25 May and 16 September at noon, respectively. In comparison with a no-coating glass, all scenarios of photochromic coated glass significantly influenced DGP. As Figures 3 and 4 illustrate, DGPs are reduced considerably by utilizing Type A, Type B, and Type C windows. The glare occurrence in the south oriented office room happened more frequently in early spring and late fall when the incidence angle was small due to low solar altitude and high intensity [55]. So, using photochromic glass in window types A, B, and C can dramatically reduce glare in the south facade during 25 May at noon, as demonstrated in Figure 3. On the other hand, as Figure 4 shows the application of photochromic glass in window types A, B, and C leads to a decrease in the negative effect of glare during 16 September at noon. However, the glare reduction is not as significant as on 25 May. In fact, sun in September would be more hamful for occupants' eyes in May since its location would be lower in the sky and at different angles that may expose the occupants to additional discomfort glare [56].

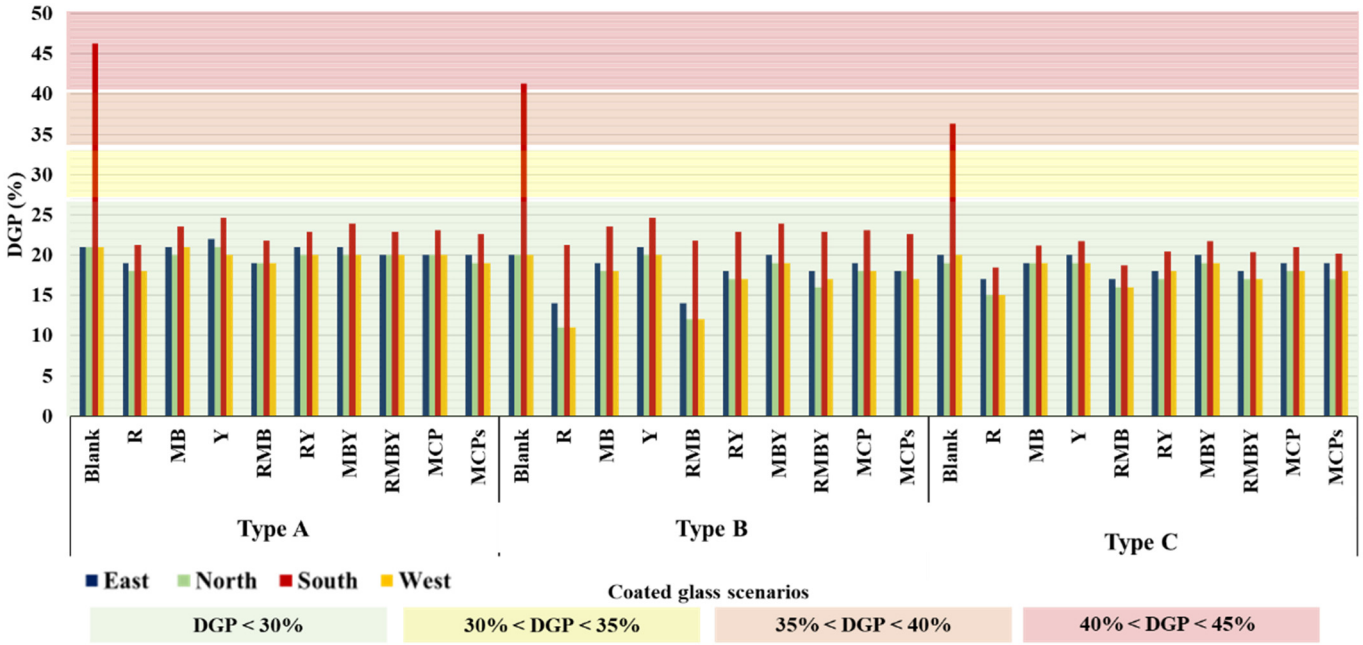

Figure 3. DGP of different color shades on 25 May at noon for four facade orientations.

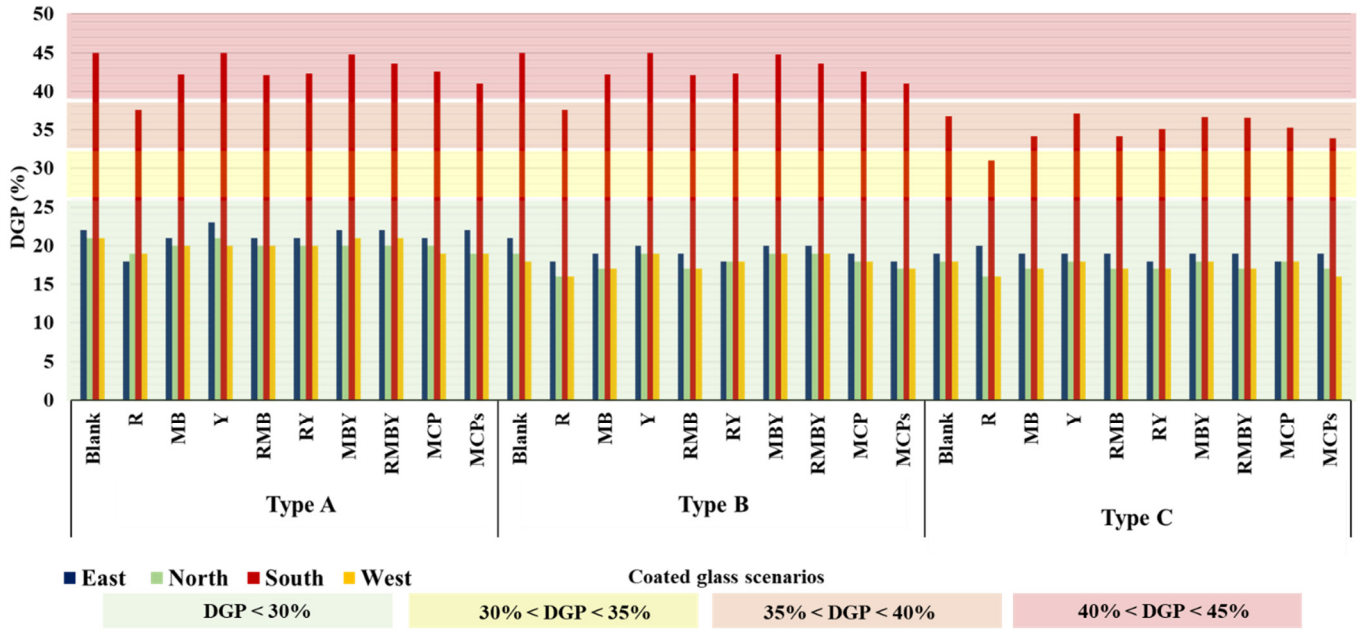

Figure 4. DGP of different color shades on 16 September at noon for four facade orientations.

Additionally, the intensity of sunlight received by west facade is in its maximum amounts during late afternoon [55]. The measurements at 6:00 p.m. on 25 May and 16 September reveal that the photochromic glass used in window types can significantly control discomfort glare in comparison with no-coating glass. Utilizing photochromic glass in all of the window types can effectively reduce glare more at 6:00 p.m. in 16 September compared to 25 May.

3.3. UDI Analysis

As well as DGP, UDI_h was also calculated for different color shades of different window types. The data was obtained on 25 May and 16 September at 12:00 p.m. and 6:00 p.m. for four cardinal orientations (N, W, S, E). Then, three ranges of UDI_{hs} were determined and recorded for further analysis. As an example, Figure 5 shows the $UDI_{underlit}$, $UDI_{overlit}$, and UDI_{useful} of all color shades in three window types on 25 May at noon in the South facade. In comparison with no-coating glass, using photochromic glass can increase UDI_{useful} percentage, decrease $UDI_{overlit}$, and increase $UDI_{underlit}$ percentage. It should be noted that decreasing $UDI_{overlit}$ can lead to less discomfort glare and increasing $UDI_{underlit}$ can lead to more of a need to use artificial light at the end of the office room [57]. Figure 5 demonstrates the useful range on 25 May at noon in a type A window with blank glass is 33, which means 33% of the working space area had useful indoor illuminance. If the R color shade was utilized, the working space area with useful indoor illuminance could increase to 44%. As a result, UDI_{useful} relatively increased by 30%. On the other hand, using the R color shade in type A can decrease $UDI_{overlit}$ and increase $UDI_{underlit}$ percentage.

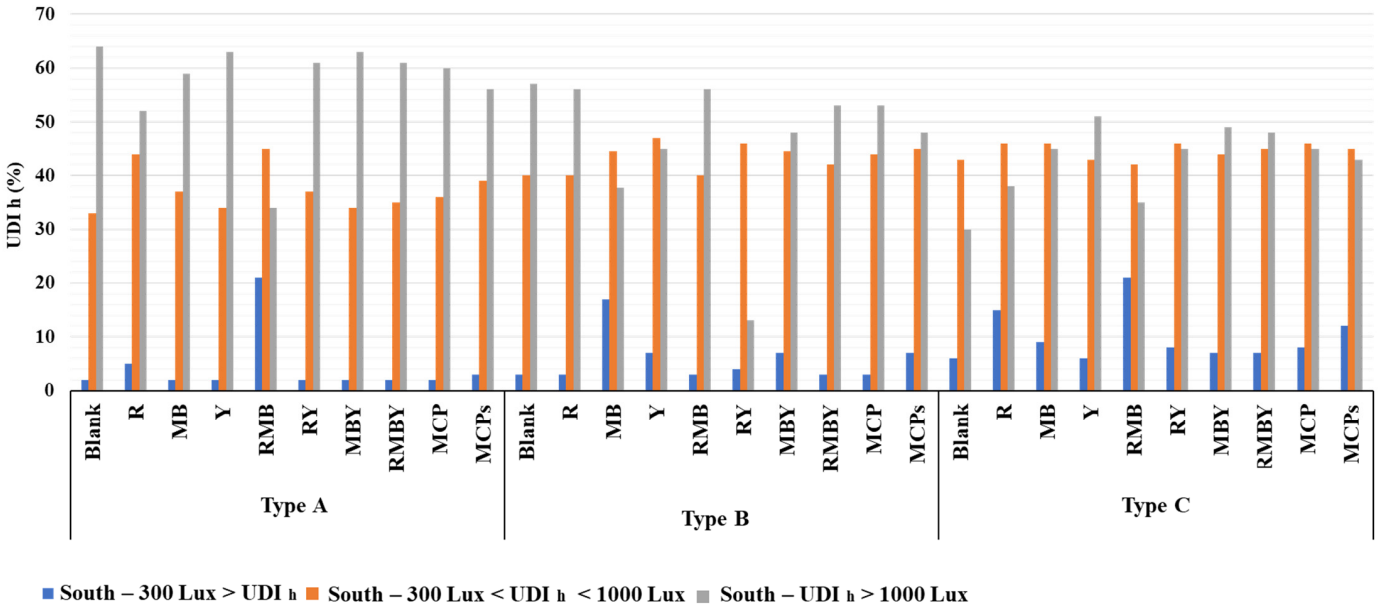

Figure 5. Three ranges of UDI_h for windowpanes for south facade orientation on 25 May at noon.

The UDI_h of different color shades utilized in each window types on 25 May and 16 September at noon for four cardinal facade directions (N, W, S, E) are demonstrated in Figures 6 and 7, respectively. As Figure 6 shows, the $UDI_{h\ acceptable}$ of south facade is lower than other facade directions in type A. Additionally, in type B the $UDI_{h\ acceptable}$ for R and RMB color shades was lower than the other color shades for all directions. As it is shown in Figure 6, there is a lower variation for different color shades and orientations in type C compared to type A and type B. As illustrated in Figure 7, the value for west orientation in all color shades and window types were higher compared to other facade orientations. In addition, big differences were observed in type C for the no-coating and MB color shade in west facade. On the other hand, the overall $UDI_{h\ acceptable}$ stands higher in type A for all color shades and orientations compared to type B and type C.

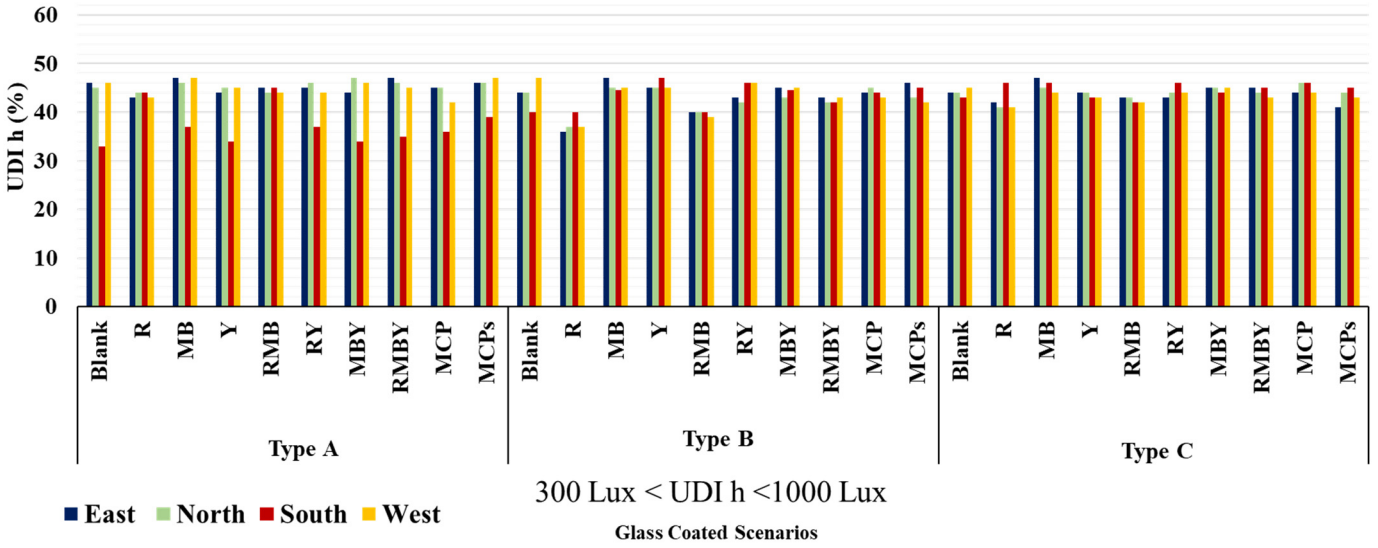

Figure 6. UDI_h of different color shades on 25 May at noon for four facade orientations.

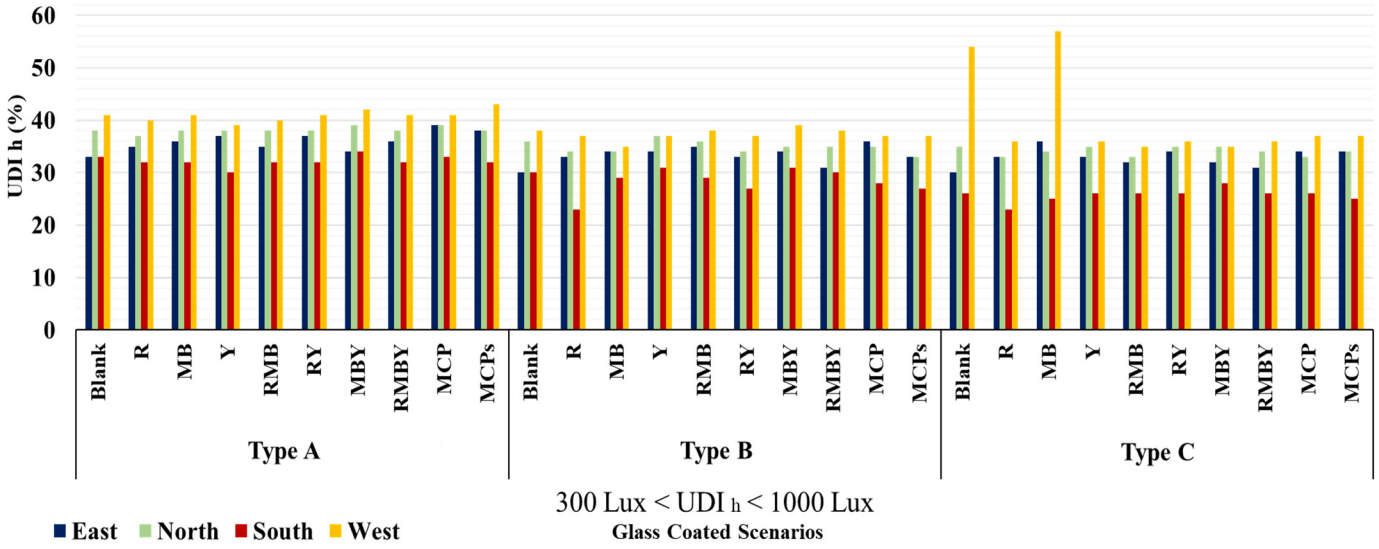

Figure 7. UDI_h of different color shades on 16 September at noon for four facade orientations.

3.4. A Comparison of Color Shades and Window Types

To identify the most effective window type and color shade in various facade orientations, the type A window was selected as a baseline for determining the average improvement rate of type B and type C by using Equations (6) and (7):

$$\text{Improvement rate of window } (j,k) = \frac{x\,(j,k) - x\,(\text{Type A},k)}{x\,(\text{Type A},k)} \times 100 \quad (6)$$

$$\text{Average Improvement rate of window Type } (j) = \sum_k \frac{\text{Improvement rate } (j,k)}{10} \quad (7)$$

where j represents either type B or type C window, k is the corresponding color shade, and x denotes either DGP or UDIh value. A sample of DGP improvement rate and its average is shown in Table 3.

Table 3. DGP improvement rate of type B and type C windows with Type A baseline on 25 May at 6:00 p.m.

		DGP Improvement Rate of Type B				DGP Improvement Rate of Type C			
		East	**North**	**South**	**West**	**East**	**North**	**South**	**West**
Photochromic Coatings Used	Blank	16%	15%	4%	17%	26%	20%	9%	21%
	R	24%	17%	13%	16%	29%	17%	18%	16%
	MB	24%	11%	11%	13%	29%	22%	14%	18%
	Y	17%	6%	6%	15%	28%	17%	12%	20%
	RMB	12%	11%	13%	13%	24%	17%	14%	18%
	RY	18%	11%	11%	15%	24%	17%	13%	15%
	MBY	12%	6%	8%	15%	24%	11%	14%	17%
	RMBY	17%	11%	9%	15%	28%	17%	13%	18%
	MCP	18%	11%	8%	13%	29%	16%	14%	15%
	MCPs	24%	11%	10%	15%	24%	17%	13%	18%
Average		18%	11%	9%	15%	26%	17%	13%	18%

Table 3 shows that type C yields better results for all color shades in all facade orientations, and also DGPs are reduced considerably by utilizing type A, type C, and type B, respectively.

Next, no-color shade was selected as a baseline to determine the improvement rate of each color shades by using Equations (8) and (9):

$$\text{Improvement rate of color shade } (i,k) = \frac{y\ (i,k) - y(\text{no} - \text{color Type A}, k)}{y\ (\text{no} - \text{color Type A}, k)} \times 100 \quad (8)$$

$$\text{Improvement rate } (i) = \sum_{k} \frac{\text{Improvement rate of color shade } (i,k)}{9} \quad (9)$$

where *i* represents a color shade, k is the corresponding window type, and y denotes either the DGP or UDI_h value. A sample of the DGP improvement rate for different color shades and its average is shown in Table 4.

Table 4. DGP improvement rate of type B and type C windows with no-color baseline on 25 May at 6:00 p.m.

		Improvement Rate of Color Shades in Type B				**Improvement Rate of Color Shades in Type C**			
		East	**North**	**South**	**West**	**East**	**North**	**South**	**West**
Photochromic Coatings Used	R	32%	25%	45%	24%	37%	25%	48%	24%
	MB	32%	20%	43%	19%	37%	30%	45%	24%
	Y	21%	15%	39%	17%	32%	25%	43%	21%
	RMB	21%	20%	44%	19%	32%	25%	45%	24%
	RY	26%	20%	43%	21%	32%	25%	45%	21%
	MBY	21%	15%	41%	17%	32%	20%	44%	19%
	RMBY	21%	20%	41%	19%	32%	25%	44%	21%
	MCP	26%	15%	41%	19%	37%	20%	45%	21%
	MCPs	32%	20%	43%	21%	32%	25%	45%	24%
Average		26%	19%	42%	20%	33%	24%	45%	22%

As shown in Table 4, type B in north direction presented the most significant improvement in DGP with color shades of MB, R, MCP, and MCPs, respectively. However, the most significant improvement in DGP in type C was observed in south with color shades of R, RMB, MCPs, MBY, respectively. The same order of DGP improvement occurred in the east and west facade directions.

Visual performance of various window types with different color shades and different facade orientations are compared in Tables 5 and 6. Table 5 presents the color shades with the highest improvement rates of DGP on 25 May and 16 September, respectively.

On 16 September at noon, type C obtained better results for all color shades in all facade orientations. DGP improved effectively in south with color shades of R, MCPs, RMB, and MCP, respectively. In north, the most significant improvement in DGP was for Type C with color shades of R, RMBY, Y, and MCPs, respectively. A similar order of DGP improvement was observed for east and west as well.

Table 5 shows the highest improvement rates of UDI_h on 25 May and 16 September. On average the acceptable UDI_h decreased for all color shades in different facade orientations if either type B or Type C were used on 25 May at 6:00 p.m., as Table 5 shows. Additonally, Type B had the maximum improvement rate with color shades of MB, RMB, CMP and CMPs in south façade direction, respectively. However, the pattern of improvement rate in the south changed when type C was used.

Table 5. Comparison of average DGP improvement rate for different facade orientations.

Day &Time	Facade Orientation	Window Type	Most Effective Color Shades
25 May 12:00 p.m.	South	Type C	R, RMB, MCPs, MBY
	North	Type C	MB, R, MCP, MCPs
	East	Type C	R, MB, MCP, MCPs
	West	Type C	R, MCPs, MB, MCP
16 September 12:00 p.m.	South	Type C	R, MCPs, RMB, MCP
	North	Type C	R, RMBY, Y, MCPs
	East	Type C	R, MCPs, RMB, MCP
	West	Type C	R, MCPs, RMB, MCP
25 May 6:00 p.m.	South	Type C	R, MB, MCPs, MCP
	North	Type C	MB, R, MCPs, MCP
	East	Type C	R, MCP, RMBY, RMB
	West	Type C	Y, MCPs, MB, R
16 September 6:00 p.m.	South	Type C	R, MB, MCPs, MCP
	North	Type C	R, MB, MCP, MCPs
	East	Type C	R, MB, MCP, MCPs
	West	Type C	R, MB, MCPs MCP

Table 6. Comparison of average UDI_h improvement rate for different facade orientations.

Day &Time	Facade Orientation	Window Type	Most Effective Color Shades
25 May 12:00 p.m.	South	Type C	RMB, MCP, MCPs, MBY
	North	Type A	MBY, MCPs, MB, MCP
	East	Type A	MB, MCPs, MCP, MBY
	West	Type A	MCPs, MB, MBY, RMBY
16 September 12:00 p.m.	South	Type B	MB, RMB, MCP, MCPs
	North	Type C	CMP, RY, CMPs, R
	East	Type C	RMB, MB, MCPs, MCP
	West	Type C	RMBY, MCPs, MCP, RMB
25 May 6:00 p.m.	South	Type A	MCP, Y, MCP, RMB
	North	Type A	MCP, MBY, MCPs, MB
	East	Type A	MCP, MCPs, RMBY, MB
	West	Type A	MCPs, MBY, Y, MCP
16 September 6:00 p.m.	South	Type C	MCP, MCPs, RMBY, MBY
	North	Type A	MCPs, RMBY, RMB, MBY
	East	Type A	MCP, RMB, RY, MCPs
	West	Type A	MBY, RMB, Y, MCP

4. Discussion

This study showed that the application of photochromic coated glass in proposed window types can control daylight discomfort effects such as glare and exceeded indoor illuminance.

Due to the smart nature of the photochromic glass, $UDI_{h\ underlit}$, $UDI_{h\ acceptable}$, $UDI_{h\ overlit}$ can be meaningfully controlled in order to provide maximum office area with less discomfort glare and less over lited/overheated conditions, along with more comfort in indoor illuminance for daily office activities, which can lead to increased occupant productivity [58]. The depth of the simulated office room was chosen to be larger than the typical depth; therefore, complementary artificial lights might be needed at the office areas far from the window, since the photochromic glass is in the opaque/colored phase at noon with high solar radiation [59].

Haghshenas et. al. [60] have suggested that by using a combination of fixed/static colored glass in windows, one can control the depth of daylight penetration in buildings. The result of this study showed that the proposed smart coated glass with real-time adaptation not only can control daylight penetration in response to daylight intensity but also can allow daylight in without blocking the view whenever it is needed. Furthermore, as it was shown in [61], applying photochromic coatings such as the proposed smart colored window types can protect interior materials and furnishings from the ultraviolet (UV) and Infrared (IR) wavelengths, which are the main reasons of discoloration and degradation.

In view of the existing drawbacks of responsive facades such as the complexity of heavy mechanical parts [62], high potential failure of material fatigue and friction [63], difficulty in parts replacement, high costs in maintenance and repairing [64], limited components durability [65], and dependency on electrical powers [64], this study suggests that a chemical-based responsive facade by using photochromic materials can overcome some of these drawbacks. The approach presented in this study could be used in early phases of practical design settings. It was shown how different color shades could be chemically formulated and evaluated from the optical characteristic perspective. Additionally, it was demonstrated that how the formulated color glasses should be evaluated based on occupants' visual comfort metrics. This study could support future researchers and designers by illustrating a full process of photochromic glass design from chemical lab experiments and optical characteristics to visual performance evaluation. The results of this study reveal that the smart window technology with photochromic coatings can be an alternative to the current products in the market.

5. Conclusions

This paper assessed the visual performance of buildings containing windows with various smart photochromic color coated glass. The colors considered were red, medium blue, yellow, and their dual and triple combinations. Three window types were designed to evaluate the performance of various color shades based on their DGP and UDI metrics.

Among different color shades, MB and its combinations such as RMB, MBY, RMBY showed the highest percentage of UDI_{useful}. The optimum performance of photochromic glass occurred in the windowpanes with MCP and MCPs colors presenting the high percentage of UDI_{useful} and the low percentage $UDI_{overlit}$. The performance of yellow photochromic glass in all window types was identical to glass with no coating.

Furthermore, all photochromic color shades had a major impact on decreasing discomfort glare by reducing the percentage of DGP values in comparison with no-coated glass. Among different color shades, R, MB, and its combinations such as RMB and RMBY had the maximum influence on controlling discomfort glare in different façade orientations, respectively. Considering both DGP and UDI metrics, colored-glass windowpanes with MCP and MCPs colors had the optimum performance in increasing useful illuminance and decreasing discomfort glare. Additonally, colored-glass windowpanes with MCP and MCPs colors have better performance in increasing useful illuminance compared to controlling discomfort glare. It needs to be mentioned that the findings of this study can open up a venue toward the applications of multi-color windowpanes such as MCP and MCPs and their possible potential in increasing visual comfort of users in various design scenarios. It needs to be noted that the optimum distributions of colors and optimum colors proportions in multi-color windowpanes must be investigated further in the future study.

Author Contributions: N.H.M.—conceptualization, methodology, analysis, draft preparation, and writing; A.E.—reviewing, validation, writing, and editing; P.M.—reviewing. All authors have read and agreed to the published version of the manuscript.

Funding: This project was funded by the Program for Research Enhancement of the Gibbs College of Architecture at the University of Oklahoma. Financial support was provided by the University of Oklahoma Libraries' Open Access Fund.

Institutional Review Board Statement: Not applicable.

Informed Consent Statement: Not applicable.

Data Availability Statement: Not applicable.

Conflicts of Interest: The authors declare no conflict of interest.

References

1. Bechthold, M.; Weaver, J.C. Materials science and architecture. *Nat. Rev. Mater.* **2017**, *2*, 17082. [CrossRef]
2. Brzezicki, M. A Systematic Review of the Most Recent Concepts in SmartWindows Technologies with a Focus on Electrochromics. *Sustainability* **2021**, *13*, 9604. [CrossRef]
3. Matin, N.H.; Eydgahi, A. Technologies Used in Responsive Facade Systems: A Comparative Study. *Intell. Build. Int.* **2020**, *12*, 54–73. [CrossRef]
4. Geoff, S.; Angus, G.; Matthew, A.; Michael, C. Nanophotonics-enabled smart windows, buildings and wearables. *Nanophotonics* **2016**, *5*, 55–73. [CrossRef]
5. Granqvist, C.G. Electrochromics and thermochromics: Towards a new paradigm for energy efficient buildings. *Mater. Today* **2016**, *3*, S2–S11. [CrossRef]
6. Gugliermetti, F.; Bisegna, F. A model study of light control systems operating with Electrochromic Windows. *Light. Res. Technol.* **2005**, *37*, 3–19. [CrossRef]
7. Seyfouri, M.M.; Binions, R. Sol-gel approaches to thermochromic vanadium dioxide coating for smart glazing application. *Sol. Energy Mater. Sol. Cells* **2017**, *159*, 52–65. [CrossRef]
8. Li, K.; Pivnenko, M.; Chu, D.; Cockburn, A.; Neill, W. Uniform and fast switching of window-size smectic A liquid crystal panels utilising thefield gradient generated at the fringes of patterned electrodes. *Liq. Cryst.* **2016**, *43*, 735–749. [CrossRef]
9. Khaligh, H.H.; Liew, K.; Han, Y.; Abukhdeir, N.M.; Goldthorpe, I.A. Silver nanowire transparent electrodes for liquid crystal-based smart windows. *Sol. Energy Mater. Sol. Cells* **2015**, *132*, 337–341. [CrossRef]
10. Meng, Q.; Wang, G.; Jiang, H.; Wang, Y.; Xie, S. Preparation of a fast photochromic ormosil matrix coating for smart windows. *J. Mater. Sci.* **2013**, *48*, 5862–5870. [CrossRef]
11. Wu, L.Y.L.; Zhao, Q.; Huang, H.; Lim, R.J. Sol-gel based photochromic coating for solar responsive smart window. *Surf. Coat. Technol.* **2017**, *320*, 601–607. [CrossRef]
12. Timmermans, G.; Saes, B.W.H.; Debije, M.G. Dual-responsive "smart" window and visually attractive coating based on a diarylethene photochromic dye. *Appl. Opt.* **2019**, *58*, 9823–9828. [CrossRef] [PubMed]
13. Li, R.; Zhou, Y.; Shao, Z.; Zhao, S.; Chang, T.; Huang, A.; Li, N.; Ji, S.; Jin, P. Enhanced Coloration/Bleaching Photochromic Performance of WO3 Based on PVP/PU Composite Matrix. *ChemistrySelect* **2019**, *4*, 9817–9821. [CrossRef]
14. Cannavale, A.; Martellotta, F.; Fiorito, F.; Ayr, U. The challenge for building integration of highly transparent photovoltaics and photoelectrochromic devices. *Energies* **2020**, *13*, 1929. [CrossRef]
15. Tällberg, R.; Jelle, B.P.; Loonen, R.; Gao, T.; Hamdy, M. Comparison of the energy saving potential of adaptive and controllable smart windows: A state-of-the-art review and simulation studies of thermochromic, photochromic and electrochromic technologies. *Sol. Energy Mater. Sol. Cells* **2019**, *200*, 109828. [CrossRef]
16. Cao, D.; Xu, C.; Lu, W.; Qin, C.; Cheng, S. Sunlight-Driven Photo-Thermochromic Smart Windows. *Sol. RRL* **2018**, *2*, 1–8. [CrossRef]
17. Miyazaki, H.; Ishigaki, T.; Ota, T. Photochromic smart windows employing WO3-based composite films. *J. Mater. Sci. Res.* **2017**, *6*, 62–66. [CrossRef]
18. Zeng, R.; Chini, A.; Srinivasan, R.S.; Jiang, P. Energy efficiency of smart windows made of photonic crystal. *Int. J. Constr. Manag.* **2017**, *17*, 100–112. [CrossRef]
19. Liang, R.; Kent, M.; Wilson, R.; Wu, Y. The effect of thermochromic windows on visual performance and sustained attention. *Energy Build.* **2021**, *236*, 110778. [CrossRef]
20. Wang, Y.; Runnerstrom, E.L.; Milliron, D.J. Switchable Materials for Smart Windows. *Annual Review of Chemical and Biomolecular Engineering.* **2021**, *7*, 283–304. [CrossRef]
21. Zou, X.; Ji, H.; Zhao, Y.; Lu, M.; Tao, J.; Tang, P.; Liu, B.; Yu, X.; Mao, Y. Research Progress of Photo-/Electro-Driven Thermochromic Smart Windows. *Nanomaterials* **2021**, *11*, 3335. [CrossRef] [PubMed]
22. Zhou, Y.; Dong, X.; Mi, Y.; Fan, F.; Xu, Q.; Zhao, H.; Wang, S.; Long, Y. Hydrogel Smart Windows. *J. Mater. Chem. A.* **2020**, *8*, 10007–10025. [CrossRef]

23. Aburas, M.; Soebarto, V.; Williamson, T.; Liang, R. Thermochromic smart window technologies for building application: A review. *Appl. Energy* **2019**, *255*, 113522. [CrossRef]
24. Cui, Y.; Ke, Y.; Liu, C.; Chen, Z.; Wang, N.; Zhang, L.; Zhou, Y.; Wang, S.; Gao, Y.; Long, Y. Thermochromic VO2 for Energy-Efficient Smart Windows. *Joule* **2018**, *2*, 1707–1746. [CrossRef]
25. Liang, R.; Wu, Y.; Wilson, R. Thermal and visual comfort analysis of an office with thermochromic smart windows applied. In Proceedings of the International Conference CISBAT 2015 Future Buildings and Districts Sustainability from Nano to Urban Scale, Lausanne, Switzerland, 9–11 September 2015; pp. 70–71.
26. Kamalisarvestani, M.; Saidur, R.; Mekhilef, S.; Javadi, F.S. Performance, materials and coating technologies of thermochromic thin fi lms on smart windows. *Renew. Sustain. Energy Rev.* **2013**, *26*, 353–364. [CrossRef]
27. Carlucci, F.; Cannavale, A.; Fiorito, F. Electrochromic window integration in adaptive building envelopes in different climates: A genetic optimization of switchable glazing parameters to reduce energy consumptions in office buildings. In *Journal of Physics: Conference Series*; IOP Publishing: Bristol, UK, 2021; Volume 2069, p. 012131.
28. Atak, G.; Pehlivan, I.B.; Montero, J.; Granqvist, C.G.; Niklasson, G.A. Electrochromic tungsten oxide films prepared by sputtering: Optimizing cycling durability by judicious choice of deposition parameters. *Electrochim. Acta.* **2021**, *367*, 137233. [CrossRef]
29. Gugole, M.; Olsson, O.; Rossi, S.; Jonsson, M.P.; Dahlin, A. Electrochromic Inorganic Nanostructures with High Chromaticity and Superior Brightness. *Nano Lett.* **2021**, *21*, 4343–4350. [CrossRef]
30. Reynisson, H. *Energy Performance of Dynamic Windows in Different Climates*; School of Architecture and the Built Environment: Stockholm, Sweden, 2015.
31. Marchwiński, J. Study of Electrochromic (EC) and Gasochromic (GC) Glazing for Buildings in Aspect of Energy Efficiency. *Archit. Civ. Eng. Environ.* **2021**, *14*, 27–38. [CrossRef]
32. Nageib, A.; Elzafarany, A.M.; Elhefnawy, M.H.; Mohamed, F.O. Using smart glazing for reducing energy consumption on existing office building in hot dry climate. *HBRC J.* **2020**, *16*, 157–177. [CrossRef]
33. Feng, W.; Zou, L.; Gao, G.; Wu, G.; Shen, J.; Li, W. Gasochromic smart window: Optical and thermal properties, energy simulation and feasibility analysis. *Sol. Energy Mater. Sol. Cells* **2016**, *144*, 316–323. [CrossRef]
34. Kazanasmaz, T.; Grobe, L.O.; Bauer, C.; Krehel, M.; Wittkopf, S. Three approaches to optimize optical properties and size of a South-facing window for spatial Daylight Autonomy. *Build. Environ.* **2016**, *102*, 243–256. [CrossRef]
35. Ekici, B.; Kazanasmaz, Z.T.; Turrin, M.; Tasgetiren, M.F.; Sariyildiz, I.S. Multi-zone optimisation of high-rise buildings using artificial intelligence for sustainable metropolises. Part 1: Background, methodology, setup, and machine learning results. *Sol. Energy* **2021**, *224*, 373–389. [CrossRef]
36. Ekici, B.Z.; Kazanasmaz, Z.T.; Turrin, M.; Tasgetiren, M.F.; Sariyildiz, I.S. Multi-zone optimization of high-rise buildings using artificial intelligence for sustainable metropolises. Part 2: Optimization problems, algorithms, results, and method validation. *Sol. Energy* **2021**, *224*, 309–326. [CrossRef]
37. González, J.; Fiorito, F. Daylight Design of Office Buildings: Optimisation of External Solar Shadings by Using Combined Simulation Methods. *Buildings* **2015**, *5*, 560–580. [CrossRef]
38. Dürr, H.; Kranz, C.; Schulz, C.; Kilburg, H.; Jönsson, H.P. Molecular and supramolecular systems in photochromism: Dihy. droindolizines—New versatile molecules. *J. Chem. Sci.* **1995**, *107*, 645–658. [CrossRef]
39. Heidari Matin, N.; Eydgahi, A.; Zareanshahraki, F. Interdisciplinary Educational Modules: Using Smart Colored Windows in Responsive Façade Systems. *Technol. Interface Int. J.* **2021**, *21*, 11–20.
40. Reinhart, C.F.; Weisman, L. The daylit area: Correlating architectural student assessments with current and emerging daylight availability metric. *Build. Environ.* **2012**, *50*, 155–164. [CrossRef]
41. Reinhart, C.F.; Jakubiec, A.; Ibarra, R. Definition of a reference office for standardized evaluations of dynamic facade and lighting technologies. In Proceedings of the Building Simulation, Chambéry, France, 25–28 August 2013; Volume 13, pp. 560–580.
42. Reinhart, C.F.; Walkenhorst, O. Validation of dynamic radiance-based daylight simulations for a test office with external blinds. *Energy Build.* **2001**, *33*, 683–697. [CrossRef]
43. Reinhart, C.F.; Andersen, M. Development and validation of a radiance model for a translucent panel. *Energy Build.* **2006**, *38*, 890–904. [CrossRef]
44. Brzezicki, M. An Evaluation of Useful Daylight Illuminance in an Office Room with a Light Shelf and Translucent Ceiling at 51° N. *Buildings* **2021**, *11*, 494. [CrossRef]
45. Brzezicki, M.; Regucki, P.; Kasperski, J. Optimization of Useful Daylight Illuminance for Vertical Shading Fins Covered by Photovoltaic Panels for a Case Study of an Office Room in the City of Wroclaw, Poland. *Buildings* **2021**, *11*, 637. [CrossRef]
46. Wienold, J.; Christo_ersen, J. Towards a New Daylight Glare Rating. In Proceedings of the 10 Europäischer Lichtkongress, Berlin, Germany, 21 September 2005; pp. 157–161.
47. Salim, F.; Khoo, C. Designing elastic transformable structures: Towards soft responsive architecture. In Proceedings of the International Conference on Computer Aided Architectural Design Research, Hong Kong, China, 27–29 April 2011.
48. Matin, N.H.; Eydgahi, A. Factors affecting the design and development of responsive facades: A historical evolution. *Intell. Build. Int.* **2020**, *12*, 1–12. [CrossRef]
49. Matin, N.H.; Eydgahi, A. A data-driven optimized daylight pattern for responsive facades design. *Intell. Build. Int.* **2021**, 1–12. [CrossRef]

50. Jakubiec, J.A.; Reinhart, C.F. A concept for predicting occupants' long term visual comfort within daylit spaces. *Leukos* **2016**, *12*, 185–202. [CrossRef]
51. Nabil, A.; Mardaljevic, J. Useful daylight illuminance: A new paradigm for assessing daylight in buildings. *Light. Res. Technol.* **2005**, *37*, 41–57. [CrossRef]
52. Nabil, A.; Mardaljevic, J. Useful daylight illuminances: A replacement for daylight factors. *Energy Build.* **2006**, *38*, 905–913. [CrossRef]
53. Mardaljevic, J. Simulation of annual daylighting profiles for internal illuminance. *J. Lighting Res. Technol.* **2000**, *32*, 111–118. [CrossRef]
54. Tabadkani, A.; Banihashemi, S.; Hosseini, M.R. Daylighting and Visual Comfort of Oriental sun Responsive Skins: A Parametric Analysis. *Build. Simul.* **2018**, *11*, 663–676. [CrossRef]
55. Hoffmann, S.; McNeil, A.; Lee, E.; Kalyanam, R. Discomfort glare with complex fenestration systems and the impact on energy use when using daylighting control. In Proceedings of Advanced Building Skins Conference, Bern, Switzerland, 3–4 November 2015.
56. Kent, M.G.; Altomonte, S.; Tregenza, P.R.; Wilson, R. Discomfort glare andtime of day. *Lighting Res. Technol.* **2014**, *47*, 641–657. [CrossRef]
57. Mardaljevic, J.; Andersen, M.; Roy, N.; Christoffersen, J. Daylighting metrics: I there a relation between useful daylight illuminanceand daylight glare probability? In Proceedings of the First Building Simulation and Optimization Conference, Loughborough, UK, 10–11 September 2012.
58. De Carli, M.; De Giuli, V.; Zecchin, R. Review on visual comfort in office buildings and influence of daylight in productivity. *Indoor Air* **2008**, *2008*, 17–22.
59. Somasundaram, S.; Chong, A.; Wei, Z.; Thangavelu, S. Energy saving potential of low-e coating based retrofit double glazing for tropical climate. *Energy Build.* **2020**, *206*, 109570. [CrossRef]
60. Haghshenas, M.; Bemanian, M.; Ghiabaklou, Z. Analysis the Criteria of Solar Trasmittance from Stained Glasses Used in Some of the Orosis from Safavid Dynasty. *J. Color Sci. Technol.* **2016**, *10*, 55–64.
61. Haghshenas, M.; Bemanian, M.; Ghiabaklou, Z. Investigating the Effect of Changing the Transmitted Light's Color on Thermal and Visual Comfort. *Naqshejahan* **2017**, *6*, 013–025.
62. Tashakori, M. Design of a Computer-Controlled Sun-Tracking Facade Model. Master Thesis, The Pennsylvania State University, State College, PA, USA, 2014.
63. Kolarevic, B.; Parlac, V. *Building Dynamics: Exploring Architecture of Change*; Routledge Press: London, UK, 2015.
64. Adriaenssens, S.; Rhode-Barbarigos, L.; Kilian, A.; Baverel, O.; Charpentier, V.; Horner, M.; Buzatu, D. Dialectic form finding of passive and adaptive shading enclosures. *Energies* **2014**, *7*, 5201–5220. [CrossRef]
65. Khoo, C.; Burry, J.; Burry, M. Soft responsive kinetic system: An elastic transformable architectural skin for climatic and visual control. In Proceeding of the Annual Conference of the Association for Computer Aided Design in Architecture, Calgary, AL, Canada, 11–16 October 2011; pp. 334–341.